Int. J. Heat Mass Transfer. Vol. 25, No. 10, pp. 1541–1558, 1982
Printed in Great Britain

0017-9310/82/101541-18 $03.00/0
Pergamon Press Ltd.

THEORETICAL AND EXPERIMENTAL INVESTIGATIONS OF I.R. RADIATION TRANSFER IN VIBRATIONALLY NONEQUILIBRATED MOLECULAR GAS CONTAINING CO_2 AND CO

N. N. KUDRYAVTSEV and S. S. NOVIKOV
Moscow Institute of Chemical Physics, USSR Academy of Sciences,
117977 Moscow, U.S.S.R.

(*Received* 12 *March* 1981)

Abstract—Radiation intensity and emissivity of the 4.3 and 2.7 μm vibrational– rotational bands of carbon dioxide and of the 4.7 μm band of carbon monoxide have been numerically calculated and experimentally measured over a wide range of parameters of vibrationally nonequilibrium mixtures expanding through the supersonic nozzle of a gasdynamic CO_2 laser. Theoretical determination of radiation characteristics of the active CO_2 laser medium in the i.r. spectral region, averaged over the rotational structure, has been made by means of the vibrational– rotational band theory using nonequilibrium energy distributions of molecules over vibrational levels reconstructed on the basis of calculations of vibrational relaxation kinetics in the mixture.

A study has been carried out of the effect made on the spectral and integral radiation and absorption of the CO_2 and CO bands under consideration by the introduction into the $CO_2 + N_2$ mixture of water molecules, essentially accelerating the processes of V–T relaxation and by the substitution of carbon monoxide for nitrogen in the $CO_2 + N_2 + He$ mixture leading to the alteration of the intermolecular $V - V'$ exchange course.

The conditions under which radiation intensity or emissivity measurements make it possible to realize reliable diagnostics of vibrational–translational and vibrational–vibrational relaxation processes occurring in a gasdynamic active laser medium have been determined.

NOMENCLATURE

A, integral emissivity [cm^{-1}];
$A(\omega)$, spectral emissivity;
B_e, rotational constant of a molecule [cm^{-1}];
$B^0(\omega, T)$, spectral blackbody radiation intensity [$W/(sterad^{-1}\ cm^2\ cm^{-1})$];
c, speed of light [$cm\ s^{-1}$];
D, geometric beam path length in a gas [cm];
d, spectral line spacing [cm^{-1}];
E_v, vibrational energy [erg];
E_r, rotational energy [erg];
F, nozzle cross-sectional area [cm^2];
g, level degeneration parity;
H_0, enthalpy value in the plenum chamber [$kcal\ mol^{-1}$];
h_*, nozzle throat height [cm];
$I(\omega)$, spectral radiation intensity [$W/(sterad\ cm^2\ cm^{-1})$];
i, subscript used to number vibrational transitions;
J, rotational quantum number;
$j(\omega)$, spectral radiation coefficient [$W/(sterad\ cm^{-1})$];
K, absorption coefficient [$atm^{-1}\ cm^{-1}$];
k, Boltzmann constant;
$\mathscr{K}$, variation of the number of quanta in the mode during vibrational transition;
l, polarization index of the CO_2 bending mode;
N, number of molecules per unit volume [cm^{-3}];
n, index used to number mixture components;
P, gas pressure [atm];
p, index for inactive (nonemitting) modes;
$Q_{ss'}$, constant of the energy exchange rate between the modes numbered with indices s and s';
Q_V, vibrational partition function;
Q_R, rotational partition function;
$R_{J''\to J'}$, matrix element of a rotational transition;
R, universal gas constant;
r, index for active (emitting) modes;
S, integrated intensity of spectral line [$atm^{-1}\ cm^{-2}$];
s, subscript used to number modes;
T_r, rotational temperature [K];
T_v, vibrational temperature [K];
T, translational temperature [K];
$T_v^{(3)}$, $T_v^{(2)}$, $T_v^{(5)}$, vibrational temperatures of asymmetric and combined modes of CO_2 and CO molecules, respectively;
U, dimensionless optical path length;
u, gas flow velocity;
v, vibrational quantum number;
W, equivalent spectral line width [cm^{-1}];

X, optical path length [atm cm];
x, empirical constant characterizing anharmonicity and interaction of modes [cm^{-1}];
y, spatial coordinate [cm];
z, dimensionless coordinate of the supersonic nozzle, $(y/h_*)\tan\varphi_0$.

Greek symbols

α, integrated intensity of vibration–rotation band [$atm^{-1}\ cm^{-2}$];
α_s, empirical constant characterizing interaction of the mode marked by the subscript s with rotation [cm^{-1}];
$\beta_{v\to v'}$, matrix element of vibrational transition;
γ, spectral line half-width [cm^{-1}];
θ_s, characteristic temperature of a mode [K];
ξ, molar concentrations;
ν, normal vibration frequency [s^{-1}];
ρ, gas density [$g\,cm^{-3}$];
$\tau(\omega)$, spectral gas transmissivity;
μ, molecular weight [$g\ mol^{-1}$];
ω, wavenumber [cm^{-1}];
ε, mean number of quanta in a mode;
$\kappa(\omega)$, spectral absorption coefficient [cm^2];
φ_0, nozzle half-angle in the throat region.

Numerals 1, 2 and 3 are used to designate the quantities related to symmetric stretching, bending and asymmetric stretching modes of CO_2, respectively. The numeral 3 is also used to number physical quantities related to the CO_2 molecule; 4, to nitrogen; 5, to carbon monoxide; 6, to water molecules and 7, to helium atoms.

INTRODUCTION

IN RECENT years, mixtures of molecular gases characterized by the nonequilibrium excitation of vibrational degrees of freedom of their molecules have been widely used in various fields of science and technology. As examples, we could note the active media of gas lasers, some reactive mixtures or gases behind shock waves and in supersonic flows which exhibit a pronounced deviation from the equilibrium between the vibrational and translational–rotational degrees of freedom [1–6].

Investigation of i.r. radiation transfer in a vibrationally nonequilibrium gas presents an important applied and scientific problem. In many cases, radiation processes have an essential effect on the energy balance of such systems. Measurements of radiation intensity or the emissivity of vibrational–rotational bands in conjunction with theoretical determination of these quantities allow the reconstruction of the distribution of molecules over vibrational levels and, hence, diagnostics of the formation mechanism of nonequilibrium energy distribution [3].

Calculation of the radiation properties of a vibrationally nonequilibrated gas under the conditions of the predominance of nonradiative energy transfer processes over the radiative ones requires the solution of two interconnected problems: the determination of the distributions of emitting molecules over vibrational levels on the basis of considering vibrational relaxation processes and the reconstruction, by means of the vibrational distributions obtained, of the radiation and absorption characteristics of the gas in the i.r. spectral region. Emission of many vibrationally nonequilibrated media, e.g. molecular laser-active mixtures, is, to a great extent, reabsorbed and characterized by an optical thickness strongly variable over the spectrum within the band [7].

In this paper, vibrationally nonequilibrated supersonic flows in gasdynamic CO_2 lasers (CO_2 – GDL) have been used to study, theoretically and experimentally, the i.r. radiation of the active medium components: CO_2 molecules in the 4.3 and 2.7 μm bands and CO molecules in the 4.7 μm band. Investigation of carbon monoxide emission is determined by the fact that these molecules are often present in substantial quantities in the active media of CO_2 lasers [1, 2, 6]. Theoretical studies have been conducted for various degrees of gas expansion in a nozzle corresponding to a variation in the value of the 'breakaway' of vibrational temperatures from the translational–rotational ones.

1. THEORETICAL CALCULATION OF THE RADIATION INTENSITY OF A PLANE LAYER OF VIBRATIONALLY NONEQUILIBRATED GAS

Investigations of i.r. radiation transfer in thermodynamically equilibrated molecular systems have been conducted [8–13]. The results obtained are widely used when determining radiation characteristics of spatially inhomogeneous gas media: planetary atmospheres [9, 11, 14], gases at high temperatures in flames [8, 12, 15], engine torches [8] etc.

The emission of a vibrationally nonequilibrated gas is characterized by a number of specific features, the most important of them being the governing influence on the medium emission properties of the populations of a considerable number of vibrational–rotational levels, and the strong reabsorption of radiation in the central parts of rotational lines with insignificant mean absorption of the gas [3]. These specific features determine the essential difference between the methods of calculation of radiation properties of a vibrationally nonequilibrated gas and those used for thermodynamically equilibrated conditions.

When determining the radiation intensity in the vibrational–rotational band of a molecular gas under the conditions considered (i.e. in the absence of an equilibrium between the vibrational and translational—rotational motions of molecules), it is necessary to establish theoretical relationships between the emitting properties of the medium in the i.r. spectrum region chosen and the distribution of nonequilibrium molecules over internal degrees of free-

dom, pressure and the translational temperature of a gas. These relationships have simple forms in the limited cases corresponding to the absence of radiation reabsorption (optically 'thin' gas layers) and to the blackbody radiation [8]. As a rule, the emission of a vibrationally nonequilibrated gas does not correspond to these limited cases. Hence, there is a necessity to carry out, when determining radiation and absorption characteristics of a gas under the conditions considered, the solution of the radiative energy transfer equation using the methods of the vibrational–rotational band theory [8–10]. Investigation of i.r. radiation transfer in a vibrationally nonequilibrated molecular gas was conducted previously in the general statement of the problem [15–17]. The radiation intensity and emissivity of vibrational–rotational bands of carbon dioxide with the assigned nonequilibrium distributions over the CO_2 vibrational modes have been determined [18–25].

The steady-state 1-dim. equation of radiative energy transfer in vibrational–rotational bands of molecular gases, provided the radiation scattering is neglected, will be [10, 26]

$$\frac{dI(\omega)}{dy} = \sum_{n,i} N_n[j_{n,i}(\omega) - \kappa_{n,i}(\omega)I(\omega)]. \quad (1.1)$$

Summation in equation (1.1) is carried out over all the mixture components and individual vibrational transitions $v' \to v$ emitting in the considered spectral region, with v' and v being the array quantum numbers of the upper and lower states, respectively.

Using the relationship between the emission and absorption coefficients $j_{n,i}(\omega) = B_{n,i}(\omega)\kappa_{n,i}(\omega)$[10, 14–16], the solution of equation (1.1) for the intensity of radiation emitted by the gas layer $0 \le y \le D$ at $I(\omega)|_{y=0} = 0$ can be written as

$$I\Big|_{y=D}(\omega) = \int_0^D \sum_{n,i} B_{n,i}(\omega)\tau(\omega)\frac{\partial \ln \tau_{n,i}(\omega)}{\partial y}dy \quad (1.2)$$

where

$$B_{n,i}(\omega) = 2hc^2\omega^3[g_{n,v'J'}N_{n,vJ}/(g_{n,vJ}N_{n,v'J'} - 1)]^{-1}, \quad (1.3)$$

$g_{n,vJ}$ are the degeneration parities of the corresponding levels,

$$\tau_{n,i}(\omega) = \exp\left[-\int_y^D N_n\kappa_{n,i}(\omega)dy'\right]$$

is the transmissivity of the gas layer $y \le y' \le D$ due to an individual vibrational transition and

$$\tau(\omega) = \prod_{i,n}\tau_{n,i}(\omega)$$

is the transmissivity due to all of the vibrational transitions.

The transmissivity of the gas layer, $\tau_{n,i}(\omega)$, and the functions $B_{n,i}(\omega)$ for each individual vibrational transition depend on the populations of the combining levels $N_{n,vJ}$ and $N_{n,v'J'}$. Therefore, the radiation intensity of a molecular gas under vibrationally nonequilibrium conditions is determined, according to equation (1.2), by the populations of a considerable number of vibrational levels, the transitions between which are within the limits of the given band. The use of the data on vibrational and rotational relaxation kinetics allows a sharp reduction to be made in the number of parameters determining the radiation intensity of a vibrationally nonequilibrated gas.

The distribution of molecules over the rotational levels is characterized by a temperature close to the translational one [6]. The distribution of molecules in the system with 5–10 lower mode levels, the transitions between which determine a major contribution to the emission of vibrationally nonequilibrated gas bands [21, 24], can be described by the Boltzmann distribution with the corresponding vibrational temperature $T_v^{(s)}$ [1, 2, 6] (the superscript s is used to number the vibration modes). The distribution of CO_2 molecules over the vibrational levels under the conditions considered can be characterized by two temperatures, $T_v^{(3)}$ and $T_v^{(2)}$, defining populations in the asymmetric and combined (symmetric and bending) modes, respectively [1, 2, 6]. Strong interaction of the symmetric and bending types of vibrations due to the Fermi resonance makes it possible to define the distribution of molecules in the symmetric and bending modes by means of the vibrational temperature alone.

Under the conditions typical of CO_2 lasers, the lower vibrational levels, $v_5 = 5$–7, of carbon monoxide are noticeably excited. The distribution of CO molecules over the lower vibrational levels in the active CO_2-laser medium is determined by the Boltzmann distribution with the vibrational temperature $T_v^{(5)}$ [1, 2, 6].

Under the conditions of low temperatures, $T = 200$–500 K, and the pressures, $P = 10^{-1}$–10^{-4} atm., characteristic of vibrationally nonequilibrated molecular systems, the rotational band widths do not exceed 10^{-2}–10^{-3} cm^{-1}. This leads to the necessity of considering, when calculating the band radiation intensities, the spectral intervals smaller by 1–2 orders of magnitude, i.e. 10^{-3}–10^{-5} cm^{-1} [7], which is a tedious task. That is why calculation of spectrum-averaged radiative and absorptive characteristics of gases in the present paper is conducted over the spectral ranges chosen equal to $\Delta\omega' = 2$–10 cm^{-1} [8–11], which corresponds to a noticeable variation (by 5–10%) of the averaged band radiation intensity. The functions $B_{n,i}(\omega)$ vary over the range $\Delta\omega'$ by no more than 1% [9].

Assuming a random spectral distribution of the combinations of rotational lines of various vibrational transitions $v' \to v$ (i.e. the statistical independence of the values of $\tau_{n,i}(\omega)$ and insignificant variations of the functions $B_{n,i}(\omega)$ over the range $\Delta\omega'$) one can obtain from equation (1.2), by means of averaging over the wavenumber, the following relationship:

$$\bar{I}_{y=D}(\omega) = \int_0^D \sum_{n,i} B_{n,i}(\omega)\bar{\tau}(\omega)\frac{\partial \ln \bar{\tau}_{n,i}(\omega)}{\partial y}dy \quad (1.4)$$

where

$$\bar{\tau}(\omega) = \prod_{i,n} \bar{\tau}_{n,i},\ \bar{I}(\omega),\ \bar{\tau}(\omega) \text{ and } \bar{\tau}_{n,i}(\omega)$$

are the values averaged by means of splitting the spectrum into the intervals $\Delta\omega'$ and calculating mean values of $I(\omega)$, τ and $\tau_{n,i}(\omega)$ over these intervals. According to equation (1.4), the calculation of radiation intensity in a vibrational–rotational band requires the determination, for each vibrational transition, of the function $B_{n,i}(\omega)$ and of the averaged transmission $\bar{\tau}_{n,i}(\omega)$.

In some cases of practical importance, the integral on the RHS of equation (1.4) can be calculated in the final form. For a gas layer of high transparency, $\bar{\tau}(\omega) \to 1$, equation (1.4) yields (see Appendix 1)

$$\bar{I}\Big|_{y=D}(\omega) = \sum_{n,i} \bar{A}_{n,i}(\omega) B_{n,i}(\omega) \qquad (1.5)$$

where $\bar{A}_{n,i}(\omega) = 1 - \bar{\tau}_{n,i}(\omega)$ is the average emissivity of the gas layer $0 \le y \le D$.

The condition $\bar{\tau}(\omega) \to 1$ is realized at small radiation absorption, $\kappa_{n,i} N_n \to 0$ ('weak' lines), and at insignificant degrees of broadening of rotational lines, when their half-widths are much smaller than the distance between the neighbouring lines (the isolated line model).

Under the conditions of thermodynamic equilibrium, the gas radiation intensity is determined by the relationship (see Appendix 2)

$$\bar{I}(\omega) = \bar{A}(\omega) B^0(\omega, T). \qquad (1.6)$$

The function

$$B^0(\omega, T) = 2hc^2\omega^3 \left[\exp\left(\frac{hc}{k}\frac{\omega}{T}\right) - 1 \right]^{-1}$$

defines the spectral distribution of blackbody radiation intensity, $\bar{A}(\omega)$ is the gas emissivity.

Equation (1.6) was used [23, 27] to determine the radiation intensity of vibrationally nonequilibrated media. In these works, the function $B^0(\omega, T)$ was calculated at the temperature equal to the vibrational temperature of the emitting mode, $T_v^{(s)}$, while the emissivity, $\bar{A}(\omega)$, was calculated taking into account the nonequilibrium distribution of molecules over the vibrational levels. A number of studies [20, 21, 24] resort to the isolated line model in order to determine the radiation intensity of a vibrationally nonequilibrated gas.

The uncertainty of determining the radiation intensity of a vibrationally nonequilibrated gas from equations (1.5) and (1.6) is illustrated in Fig. 1(a) for the 4.3 μm CO_2 band, and in Fig. 1(b) for the 4.7 μm CO band. The vibrationally nonequilibrated gas parameters used in these calculations are given in the figure

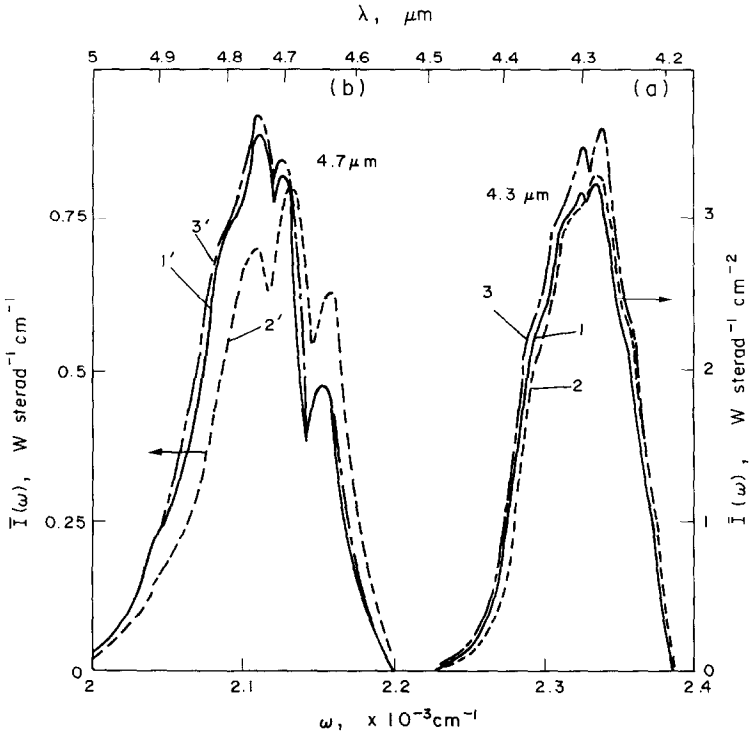

FIG. 1. Spectral radiation intensity, $\bar{I}(\omega)$ in the 4.3 μm CO_2 bands (a) curves 1–3, and 4.7 μm CO bands (b) curves 1′–3′. Curves 1 and 1′ present the calculation results on equation (1.3) obtained in this paper, 2 and 2′ on equation (1.5) accounting for nonequilibrium molecules distribution over vibrational levels, 3 and 3′, according to the model assuming the weak radiation absorption, $\bar{\tau}(\omega) \to 1$, equation (1.4). Calculation of the radiation intensity in the 4.3 μm band has been done for the mixture 10% CO_2 + 90% N_2 at $T = 300$ K, $T_v^{(2)} = 500$ K, $T_v^{(3)} = 1500$ K, $P = 10^{-2}$ atm, $X = 4.5 \times 10^{-2}$ atm cm; in the 4.7 μm band, for the mixture 10% CO + 90% N_2 at $T = 100$ K, $T_v^{(5)} = 2000$ K, $P = 10^{-2}$ atm, $X = 2 \times 10^{-2}$ atm cm.

caption. It can be seen that in the case of the 4.3 μm band, the values of spectral radiation intensity calculated from equation (1.6) differ from those obtained by accurate calculation from equation (1.4) by no more than 5% (curves 1 and 2 in Fig. 1a). Determination of the spectral radiation intensity from equation (1.5), valid at $\bar{\tau}(\omega) \to 1$, leads to overestimation of the calculation results for radiation intensity by no more than 10–15% as compared with calculation by equation (1.4) (curves 1 and 3 in Fig. 1a). The error in determining the spectrum-integrated radiation intensity of the 4.3 μm band from equations (1.5) and (1.6) is 2–3 times smaller than the error obtained when calculating the spectral characteristics of this band's radiation by equations (1.5) and (1.6) and does not exceed 5%. These approximate equations yield nearly the same error when calculating the radiation intensity of the 4.7 μm CO band under the gas parameters displayed in Fig. 1(a).

With a decrease in the translational temperature, T, to 100 K (Fig. 1b), the use of the approximate relationship (1.5) leads to errors reaching 25–30% when determining the spectral characteristics, and 5–10% when determining the integral characteristics of the 4.7 μm emission band (curves 1 and 2 in Fig. 1b). A smaller error is obtained under these conditions by means of using the relationship corresponding to weak absorption (curve 3 in Fig. 1b).

The parameters of the vibrationally nonequilibrated CO_2 – GDL media studied in this paper correspond to the data given in Fig. 1(a). Therefore, proceeding from the results obtained, the radiation intensity of CO_2 and CO molecules was determined on the basis of relation (1.6) allowing for the nonequilibrium distribution of molecules over the vibrational levels.

2. DETERMINATION OF THE SPECTRUM-AVERAGED GAS TRANSMISSIVITY

It has been shown earlier that the calculation of the radiation intensity of vibrationally nonequilibrated gas is reduced to the determination of the functions $B_{n,i}(\omega)$ and the transmissivity $\bar{\tau}_{n,i}(\omega)$ for each vibrational transition forming a band. The functions $B_{n,i}(\omega)$ are calculated from relation (1.3). Determination of the spectrum-averaged transmissivity, $\bar{\tau}_{n,i}(\omega)$, is carried out using the models of vibrational–rotational bands [8–11].

In the present paper, the model [9, 10] was used, which implies the statistical distribution of rotational lines over the averaging interval $\Delta\omega'$. The rotational line intensity for each individual vibrational transition $v \to v'$ over the wavenumber range $\Delta\omega' = 2\text{–}10\,\text{cm}^{-1}$ was assumed constant and equal to the corresponding mean value. The error in determining the transmissivity by the adopted model does not exceed 10% [10].

In the statistical model of line distribution over the spectrum, the mean transmissivity is determined [8] by

$$\bar{\tau}_{n,i}(\omega) = \exp\left[-\sum_{n,i} W_{n,i}(\omega)/d_{n,i}(\omega) \right], \qquad (2.1)$$

in which

$$W_{n,i}(\omega) = \int_{-\infty}^{\infty} \{1 - \exp[-K_{n,i}(\omega)X]\}\, d\omega$$

is the equivalent width of rotational lines, $d_{n,i}(\omega)$ is the distance between the centers of the neighbouring lines of an individual vibrational transition, $K(\omega)$ the absorption coefficient, $X = P_n D$ the optical thickness of the emitting volume and P_n the partial pressure of the emitting mixture component.

The profile of rotational lines under the conditions typical of vibrationally nonequilibrated systems is determined by the combined effect of the Doppler and collision mechanisms of broadening. Under these conditions, the spectral form of rotational lines is described by the Voigt function. The equivalent width of lines with the Voigt profile can be determined within 8% from [28]

$$W_F = [W_L^2 + W_D^2 - (W_L \cdot W_D/SX)^2]^{1/2}, \quad (2.2)$$

where $W_L = W_L(U_L)$ and $W_D = W_D(U_D)$ are the equivalent widths corresponding to the collisional and Doppler broadening mechanisms,

$$S = \int_{-\infty}^{\infty} K(\omega)\, d\omega$$

is the integrated intensity of the line. The dimensionless parameters

$$U_L = \frac{SX}{2\pi\gamma_L} \quad \text{and} \quad U_D = \frac{SX}{\pi^{1/2}\gamma_D}$$

characterize one half of the optical path length in the center of lines with collisional and Doppler profiles, γ_L and γ_D are the corresponding half-widths of the lines. The equivalent widths $W_L(U_L)$ and $W_D(U_D)$ at arbitrary optical thicknesses can be determined, with a relative error not exceeding 10^{-6}, from approximating relations [28] in the form of exponential polynomials over U_L and U_D, respectively.

The integral intensity of the vibrational–rotational line, corresponding to the rotational, $J \to J'$, and vibrational, $v \to v'$, transitions for diatomic and 'parallel' bands of linear triatomic molecules is given by [8]

$$S_{vJ \to v'J'} = \sigma \frac{N_{vJ}}{N_v} \frac{\omega_{vJ \to v'J'}}{\omega_{v \to v'}} \times S_{v \to v'}(R_{J \to J'})^2 \frac{\left(1 - \dfrac{g_{vJ}N_{v'J'}}{g_{v'J'}N_{vJ}}\right)}{\left(1 - \dfrac{g_v N_{v'}}{g_{v'}N_v}\right)} \qquad (2.3)$$

where $(R_{J \to J'})^2$ is the matrix element square of the rotational transition $J \to J'$, $\sigma = 1$ for CO and for the CO_2 transitions with $l \geq 1$, $\sigma = 2$ for CO_2 transitions with $l = 0$, $\omega_{vJ \to v'J'}$ is the wavenumber in the rotational line center, $\omega_{v \to v'}$ the wavenumber corresponding to the 'transition' involving variation of the quantum numbers $v \to v'$ and $J = J' = 0$, $S_{v \to v'}$ is the integrated

intensity of the vibrational transition $v \to v'$ written as [8]

$$S_{v\to v'} = \frac{8\pi}{3hc}\frac{N_v}{P}\omega_{v\to v'}\beta^2_{v\to v'}\left(1 - \frac{g_v N_{v'}}{g_{v'} N_v}\right), \quad (2.4)$$

with $\beta_{v\to v'}$ being the vibrational transition matrix element. The dependence of the matrix element $\beta_{v\to v'}$ on the quantum numbers $v = v_1 \ldots v_n$ is determined theoretically [8]. This makes it possible to calculate the value of $S_{v\to v'}$ for transitions between the excited states on the basis of the measured integrated intensity of the whole vibrational–rotational band under normal conditions, α_0, ($P_{st} = 1.0$ atm., $T_{st} = 293$ K), when

$$\alpha_0 = \sum_{v,v'} S_{v\to v'} = S_{0\to 1}.$$

According to the adopted model of vibrational and rotational relaxation processes, the populations of vibrational and vibrational–rotational levels are given by

$$N_v = Q_v^{-1}\prod_s g_v^{(s)} \exp\left[-E_v^{(s)}/kT_v^{(s)}\right], \quad (2.5)$$

$$N_{vJ} = N_v Q_R^{-1}(2J+1)\exp\left[-E_r/kT\right]$$

where

$$Q_v = \prod_s \left[1 - \exp(-\theta_v^{(s)}/T_v^{(s)})\right]^{-g_v^{(s)}}$$

$$Q_R = \frac{k}{hc}\frac{T}{B_e}$$

are the vibrational and rotational partition functions, $g_v^{(s)}$ is the degeneration parity of the mode numbered with the superscript s.

The anharmonicity of a molecule and the constant characterizing interaction of various modes, in cm^{-1}, are comparable with the spectral range, within which the rotational lines of the individual vibrational transitions $v \to v'$ are situated at low gas temperatures, $T \leq 300$ K. Moreover, the distribution of rotational lines of the vibrational transition $v \to v'$ over the spectrum is, to a great extent, governed by the interaction between the molecular vibrations and rotation. Therefore, the vibrational and rotational energies should be determined using the empirical relationships which account for the above factors [8, 10]

$$E_v^{(s)} = \sum_s \nu_e^{(s)}\left(v_s + \frac{g_v^{(s)}}{2}\right) - \sum_{\substack{s,s' \\ s' \geq s}} x_{ss'}\left(v_s + \frac{g_v^{(s)}}{2}\right)\left(v'_s + \frac{g_v^{(s')}}{2}\right), \quad (2.6)$$

$$E_r = J(J+1)\left[B_e - \sum_s \alpha_s\left(v_s + \frac{g_v^{(s)}}{2}\right)\right],$$

where $\nu_e^{(s)}$, $x_{ss'}$, α_s are the empirical constants defining the molecular normal vibration frequency, anharmonicity and interaction of various types of vibrations and interaction between the molecular vibrations and rotation, respectively. Equation (2.6) yields the relationship defining the distribution of rotational lines of the vibrational transition $v \to v'$

$$\omega_{vJ\to v'J'} = \omega_{v\to v'} + 2B_e m - \sum_s \alpha_s\left[m(m+1)\Delta v_s + 2m\left(v_s + \frac{g_v^{(s)}}{2}\right)\right], \quad (2.7)$$

in which $m = J + 1$ for the R-branch and $m = -J$ for the P-branch, Δv_s is the variation of the number of quanta in the mode numbered with the index s. Equation (2.7) yields

$$m = \frac{F \pm [F^2 - C(\omega_{vJ\to v'J'} - \omega_{v\to v'})]^{1/2}}{C}, \quad (2.8)$$

where

$$F = B_e - \frac{C}{2} - \sum_s \alpha_s\left(v_s + \frac{g_v^{(s)}}{2}\right), \; C = \sum_s \alpha_s \Delta v_s.$$

If m is taken to be a continuously changing parameter, then it can be assumed in equation (2.8) that $\omega_{vJ\to v'J'} = \omega$. The minus sign in equation (2.8) corresponds to the P-branch lines and to the R-branch lines up to the edge, the plus sign, to the R-branch lines after the edge [29]. Equation (2.8) yields the relationship determining the distance between the neighbouring rotational lines

$$d(\omega) = [F^2 - C(\omega - \omega_{v\to v'})]^{1/2}. \quad (2.9)$$

For the vibrational states of CO_2 with the stretching mode polarization index $l = 0$, half of the rotational states are forbidden. That is why the value of $d(\omega)$ doubles during transitions between these states as compared with the corresponding value determined from equation (2.9).

Thus, relations (2.8) and (2.9) allow all the parameters, which are necessary for calculation of the averaged transmissivity and which are dependent on the rotational quantum number J, to be made dependent on the wavenumber ω.

In the CO_2 vibrational transitions, corresponding to the polarization index of the bending model $l > 0$, the Q-branches are also present. The radiation intensity of the entire Q-branch in the 'parallel' CO_2 vibrational transitions is of the same order as the radiation value of one intensive rotational line of P- and R-branches [30]. Therefore, radiation in the Q-branches in the 'parallel' bands of CO_2—4.3 and 2.7 μm—are not taken into account in the present work.

Determination of the Doppler half-width of rotational lines was carried out using the relationship

$$\gamma_D = \left(\frac{\omega_{vJ\to v'J'}}{C}\right)\left[\frac{RT\ln 2}{\mu}\right]^{1/2}$$

where μ is the molecular weight of all emitting molecules. Calculation of the partial collisional half-width $\gamma_L^{(n)}$, which characterizes the interaction of the emitting molecule with the mixture components numbered with the superscript n, involves certain difficulties due to the insufficient experimental data on

Table 1. The values of parameters of the studied bands and transitions forming them, which were used in the calculations

No.	Parameters		Band 4.7 μm	4.3 μm	2.7 μm
1.	Variation of vibrational quantum numbers during transition		$v_5 + 1 \to v_5$	$v_1 v_2^l v_3 + 1 \to v_1 v_2^l v_3$	(a) $v_1 + 1 v_2^l v_3 + 1$ (b) $v_1 (v_2 + 2)^l v_3 + 1$ $\to v_1 v_2^l v_3$
2.	Dependence of the matrix element square on vibrational quantum numbers		$v_5 + 1$ [8]	$v_3 + 1$ [8]	$(v_1 + 1)(v_3 + 1)$ [37]
3.	Dependence of the matrix element square on rotational quantum numbers		$\lvert m \rvert$ [8]	$\left\lvert \frac{(m)^2 - (l)^2}{m} \right\rvert$ [8]	$\left\lvert \frac{m^2 - l^2}{m} \right\rvert$ [8]
4.	Integrated intensity of the band under normal conditions in α_0 (atm^{-1} cm^{-2})		239 [10, 32]	2700 [8, 10]	(a) 39.3 (b) 25.7 [10, 33]
5.	Parameters in equations (2.8) and (2.9)	F	$B_e^{(5)} - \alpha_5(v_5 + 1)$ [38]	$B_e^{(3)} - \alpha_1(v_1 + 1/2) - \alpha_2(v_2 + 1) - \alpha_3(v_3 + 1)$ [29]	(a) $B_e^{(3)} - \alpha_1(v_1 + 1) - \alpha_2(v_2 + 1) - \alpha_3(v_3 + 1)$ (b) $B_e^{(3)} - \alpha_1(v_1 + 1/2) - \alpha_2(v_2 + 2) - \alpha_3(v_3 + 1)$ [29]
		C	α_5 [38]	α_3 [29]	(a) $\alpha_1 + \alpha_3$ (b) $2\alpha_2 + \alpha_3$ [29]
6.	Mean collisional half-widths under normal conditions $\gamma_{L,st}^{(n)}$, atm^{-1} cm^{-1} for $M = CO_2$, N_2, CO, He and H_2O	CO_2	0.072 [32, 34, 35]	0.087 [31, 36, 39]	0.087*
		N_2	0.06 [32, 34, 35]	0.0670 [31, 36, 39]	0.067*
		CO	0.060 [32, 34, 35]	0.067 [31, 36, 39]	0.067*
		He	0.040 [32, 34, 35]	0.040 [31, 36, 39]	0.040*
		H_2O	0.060 [10]	0.042 [10]	0.042*

* Collisional half-widths in the 2.7 μm band were assumed to be the same as in the 4.3 μm band [31, 36].

Table 2. Spectroscopic constants of CO and CO_2 molecules [8, 10, 38, 40]

Spectroscopic constants		CO_2 Symmetric ν_1	CO_2 Bending ν_2	CO_2 Asymmetric ν_3	CO
$\nu_e^{(s)}$	cm^{-1}	1354.9	673.0	2396.5	2170.2
B_e	cm^{-1}		0.391635		1.93139
α_s	cm^{-1}	0.0012	−0.00072	0.0030825	0.017485
$x_{ss'}\cdot cm^{-1}$	ν_1	3.75	−3.65	19.73	
	ν_2		0.63	12.53	13.461
	ν_3			12.63	
θ_s	K	1923.8	960.5	3382.6	3090.0

broadening of different rotational lines of the bands over the studied pressure range, $P = 10^{-4}$–10^{-1} atm., and the gas temperature range, $T = 300$–2000 K.

The dependence of partial collisional half-widths, $\gamma_L^{(n)}$, on the type of vibrational transition and excitation of combining levels is insignificant [31]. In the region of low gas temperatures, $T \lesssim 300$ K, the emitting molecule rotational state has a substantial effect on $\gamma_L^{(n)}$ [31]. In the calculations conducted in this study, partial collisional half-widths, $\gamma_L^{(n)}$, of the CO_2 and CO bands were used averaged with respect to the rotational quantum number J recommended by various authors [10, 31–36, 39] and given in Table 1.

In order to determine the collisional half-widths in gas mixture at arbitrary pressures and temperatures, the following theoretical relation was used [8]

$$\gamma_L = P\left[\frac{T_{st}}{T}\right]^{1/2} \sum_n \xi_n \gamma_{L,st}^{(n)} \qquad (2.10)$$

where $\gamma_{L,st}^{(n)}$ are the values of $\gamma_L^{(n)}$ under normal conditions, ξ_n are the molar concentrations of components. Calculations of the 4.3 μm CO_2 and 4.7 μm CO band radiation with the use of the minimum and maximum collisional half-widths $\gamma_L^{(n)}$ depending on the rotational quantum number J [10, 31, 34–36, 39] yield, at the minimum temperatures studied in this paper ($T = 300$ K) a discrepancy not exceeding 15%. It can be expected, therefore, that the maximum calculation error, when using the mean values of $\gamma_L^{(n)}$, is about half as large and decreases with an increase in the gas temperature T.

The values of the parameters of the bands considered and of the transitions which form them, used when calculating the radiation intensity, are given in Fig. 1, while the spectroscopic constants of CO and CO_2 molecules, in Table 2.

3. CALCULATION OF VIBRATIONAL TEMPERATURES IN GAS NOZZLE FLOW

Calculation of vibrational temperatures for the conditions under study requires solution of gasdynamic equations in conjunction with the vibrational relaxation ones. Gasdynamic equations for the process of 1-dim. isentropic expansion of the CO_2 – GDL mixture possibly containing five components: CO_2, N_2, CO, He and H_2O, were written in the following form [41]

$$\rho u F = \text{const}, \quad \rho u \frac{du}{dx} = -\frac{dP}{dx},$$

$$\left(\frac{5}{2} + \sum_{n=3}^{6} \xi_n + \frac{1}{2}\xi_6\right) RT + R\left(\xi_3 \sum_{s=1}^{3} \theta_s \varepsilon_s + \sum_{s=4}^{5} \xi_s \theta_s \varepsilon_s\right) + \frac{\mu u^2}{2} = H_0 \qquad (3.1)$$

where

$$\mu = \sum_{n=1}^{7} \xi_n \mu_n,$$

$$\varepsilon_6 = [\exp(-\theta_v^{(s)}/T_v^{(s)}) - 1]^{-1}$$

is the mean number of vibrational quanta in the mode numbered with the superscript s. The subscript '6' is used to denote the physical quantities related to the H_2O molecules, the index 7, to the He atoms.

It was assumed that in the $CO_2 + N_2 + CO + He(H_2O)$ mixture, the following vibrational energy exchange processes occur:

V–T relaxation of the combined CO_2 mode [1, 2, 6]

$$CO_2(01^10) + M \overset{Q_{20}}{\rightleftarrows} CO_2(00^00) + M + k\theta_2; \quad (3.2)$$

intermolecular V–V' exchange in carbon dioxide

$$CO_2(00^01) + M \overset{Q_{32}}{\rightleftarrows} CO_2(mr^l0) + M + \Delta E_{32}, \quad (3.3)$$

where $m = 0, r = 3, l = 0$ or $m = r = 1, \Delta E_{32} = (\theta_3 - 3\theta_2)k$ at $T < 1400$ K and $m = 0, r = 2, l = 0$ or $m = 1$, $r = l = 0, \Delta E_{32} = (\theta_3 - 2\theta_2)$ at higher temperatures;

V–V' exchange between the asymmetric CO_2 mode and N_2, CO molecules

$$N_2(1) + CO_2(00^00) \overset{Q_{34}}{\rightleftarrows} N_2(0) + CO_2(00^01) + (\theta_4 - \theta_3)k, \quad (3.4)$$

$$CO(1) + CO_2(00^00) \overset{Q_{35}}{\rightleftarrows} CO(0) + CO_2(00^00) + (\theta_5 - \theta_3)k, \quad (3.5)$$

$$N_2(1) + CO(0) \overset{Q_{45}}{\rightleftarrows} N_2(0) + CO(1) + (\theta_4 - \theta_5)k; \quad (3.6)$$

V–V' exchange between the bending CO_2 mode and CO molecule

$$CO(1) + CO_2(00^00) \overset{Q_{52}}{\rightleftarrows} CO(0) + CO_2\begin{pmatrix}11^10\\03^10\end{pmatrix} + (\theta_5 - 3\theta_2)k \quad (3.7)$$

V–T relaxation of N_2 and CO molecules

$$N_2(1) + M \overset{Q_{40}}{\rightleftarrows} N_2(0) + M + k\theta_4, \quad (3.8)$$

$$CO(1) + M \overset{Q_{50}}{\rightleftarrows} CO(0) + M + k\theta_5, \quad (3.9)$$

where

$$Q_{ss'} = \sum_n \xi_n Q_{ss'}^{(n)}$$

in the gas mixture.

According to the adopted scheme of vibrational relaxation processes, the equations describing variation of ε_s are [1, 6]:

$$\begin{aligned}
u\frac{d\varepsilon_5}{dx} &= \xi_4\varphi_{45} + \xi_3\varphi_{35} - \frac{1}{8}\xi_3\varphi_{52} - \varphi_{50},\\
u\frac{d\varepsilon_4}{dx} &= \xi_3\varphi_{34} - \xi_5\varphi_{45} - \varphi_{40},\\
u\frac{d\varepsilon_3}{dx} &= -\xi_4\varphi_{34} - \xi_5\varphi_{35} - \frac{1}{8}\varphi_{32},\\
u\frac{d\varepsilon_2}{dx} &= v\left[\frac{1}{8}(\mathscr{K}\varphi_{32} + 3\xi_5\varphi_{52}) - \varphi_{20}\right],
\end{aligned} \quad (3.10)$$

where

$$\varepsilon_1 = \varepsilon_2^2/[4(\varepsilon_2 + 1)],$$

$$v = 2(\varepsilon_2 + 1)^2/(3\varepsilon_2^2 + 6\varepsilon_2 + 2),$$

$$\varphi_{ss'} = PQ_{ss'}\{\varepsilon_s(\varepsilon_{s'} + 1) - \varepsilon_{s'}(\varepsilon_s + 1)\exp[(\theta_{s'} - \theta_s)/T]\},$$

$$(s, s') = (4,5), (3,5), (3,4),$$

$$\varphi_{32} = PQ_{32}\{\varepsilon_3(\varepsilon_2 + 2)^{\mathscr{K}} - \varepsilon_2^{\mathscr{K}}(\varepsilon_3 + 1)\exp[(\mathscr{K}\theta_2 - \theta_3)/T]\},$$

$$\mathscr{K} = 3 \quad \text{at} \quad T \leq 1400\,\text{K},$$

$$\mathscr{K} = 2 \quad \text{at} \quad T > 1400\,\text{K}.$$

The measured rate constants of V–T relaxation processes of CO and N_2 [equilibria (3.8) and (3.9)] at various temperatures were approximated by means of the Landau–Teller-type relationship $-\lg Q_{s_0}^{(n)} = a_s^{(n)} T^{-1/3} + b_s^{(n)}$. The values of the coefficients $a_s^{(n)}$ and $b_s^{(n)}$ are given in Table 3. The experimental data on rate constants of the V–V' [equilibria (3.3)–(3.6)] and V–T [equilibrium (3.2)] relaxation of CO_2 are presented for the gas temperatures 125 K $\leq T \leq$ 3000 K in Table 4. Velocity constants at arbitrary temperatures were determined by quadratic interpolation with respect to the parameter $T^{-1/3}$.

Experimental values of the rate constant of the process (3.7), Q_{52}, over the studied temperature range are evidently absent at present. The rate constant Q_{52} at room temperature is given in refs. [60, 65]. The values of Q_{52} obtained are close to the rate constant of the CO_2 combined mode deactivation in collisions of CO_2 with CO, $Q_{32}^{(5)}$. Therefore, it is assumed in this paper that $Q_{52} = Q_{32}^{(5)}$ for all the temperatures considered.

Integration of the system of gasdynamic (3.1) and kinetic (3.10) equations was carried out using an automatic step choice. The integration was begun behind the critical point situated downstream at the distances from the nozzle throat plane smaller than x = 0.1–0.2 mm [1]. The gas flow up to the critical point was assumed to be in equilibrium.

Table 3. The values of the coefficients $a_s^{(n)}$ and $b_s^{(n)}$ to calculate the $V - T$ relaxation rate constants for N_2 and CO molecules (in μs at P = 1.0 atm.) according to the Landau–Teller-type relationship $-\lg Q_{s0}^{(n)} = a_s^{(n)} T^{-1/3} + b_s^{(n)}$

Rate constants		$Q_{40}^{(n)}$			$Q_{50}^{(n)}$		
M	Temperature range	$a_4^{(n)}$	$b_4^{(n)}$	Reference	$a_5^{(n)}$	$b_5^{(n)}$	Reference
CO_2	200–3000	104	−5.20	[42]	75.8	−4.16†	
N_2	200–3000	104	−5.19	[42,43]	75.8	−4.16†	
CO	200–3000	104	−5.19*		75.8	−4.16	[43,44]
He	200–3000	56.2	−3.85	[42]	22.5	−1.50	[45,46]
	350–3000	56.2	−3.85	[42]	39.4	−2.52	[43]
H_2O	200–3000	36.8	−3.81	[42,43,48]	36.8	−4.81	[47]

* The efficiency of CO molecules during nitrogen deactivation was assumed the same as that of N_2 molecules.

† The efficiency of CO_2 molecules during CO vibrations deactivation was assumed the same as that of carbon monoxide molecules.

Table 4. Values of logarithms of rate constants of vibrational relaxation processes (3.2)–(3.6) in μs^{-1} at $P = 1.0$ atm. as functions of gas temperatures for gases M

Rate constant		$\lg Q_{32}^{(n)}$					$\lg Q_{20}^{(n)}$					$\lg Q_{34}$	$\lg Q_{35}$	$\lg Q_{45}$
T (K)	$T^{-1.3}$	CO_2	N_2	CO	He	H_2O	CO_2	N_2	CO	He	H_2O			
2915	0.07	1.57	1.30	1.32	1.13	0.90	1.04	1.10	0.04	0.87	1.00	0.51	1.35	0.70
1953	0.08	1.25	1.00	1.00	0.78	0.98	0.78	0.75	−0.12	0.86	1.16	0.25	1.24	0.00
1372	0.09	0.92	0.63	0.67	0.40	1.05	0.50	0.40	−0.27	0.86	1.32	0.20	1.12	−0.25
1000	0.10	0.60	0.21	0.35	0.00	1.13	0.25	0.10	−0.42	0.85	1.48	0.34	1.02	−0.27
751	0.11	0.27	−0.17	0.00	−0.40	1.23	0.00	−0.18	−0.58	0.79	1.65	0.48	0.89	−0.30
579	0.12	−0.10	−0.51	−0.28	−0.78	1.29	−0.24	−0.41	−0.73	0.74	1.87	0.65	0.83	−0.35
455	0.13	−0.37	−0.76	−0.57	−1.00	1.29	−0.44	−0.66	−0.87	0.64	2.11	0.80	0.75	−0.38
364	0.14	−0.55	−0.94	−0.66	−1.16	1.31	−0.62	−0.85	−1.02	0.54	2.36	0.95	0.68	−0.43
296	0.15	−0.61	−1.06	−0.75	−1.24	1.32	−0.76	−1.07	−1.18	0.43	2.57	1.08	0.62	−0.45
244	0.16	−0.61	−1.14	−0.77	−1.34	1.33	−0.80	−1.25	−1.24	0.32	2.57	1.41	0.61	−0.49
203	0.17	−0.54	−1.18	−0.69	−1.40	1.33	−0.82	−1.40	−1.48	0.23	2.95	1.45	0.69	−0.52
171	0.18	−0.42	−1.21	−0.54	−1.45	1.33	−0.82	−1.55	−1.63	0.12	3.15	1.48	0.74	−0.56
146	0.19	−0.27	−1.22	−0.39	−1.48	1.33	−0.82	−1.70	−1.80	0.02	3.35	1.60	0.85	−0.59
125	0.20	−0.12	−1.23	−0.23	−1.49	1.33	−0.82	−1.84	−1.95	−0.10	3.54	1.74	0.98	−0.63
References		[49,50]	[49,51]	[51,52]	[49,50]	[53,54]	[55–58]	[55,57]	[59,60]	[55]	[42,61]	[42,51, 57,59, 62]	[51,57, 58,59, 62,63]	[59, 64]

4. RESULTS OF CALCULATION OF RADIATION INTENSITY AND EMISSIVITY OF A VIBRATIONALLY NONEQUILIBRIUM GAS

In this paper, while determining the radiation and absorption characteristics of the gas, we considered rotational levels with populations exceeding 10^{-5} with respect to the corresponding value of the maximum populated rotational state of the ground vibrational level of the molecule. At the characteristic values of the rotational, $T_r = 300$ K, and vibrational, $T_v = 1000$–2000 K, temperatures, this leads to the necessity of taking into account 30–60 rotational and 5–10 vibrational levels in each mode.

For each individual vibrational transition forming a band, the radiation transfer in the P-branch lines and R-branch lines up to the edge was taken into account. The calculations show that the gas radiation intensity behind the edge of the vibrational transition decreases rapidly with the rotational temperature T_r and does not exceed 2–3% of radiation in the P- and R-branches up to the edge at the characteristic temperature $T = 300$ K.

The integral radiation intensity and emissivity of bands was determined over the spectral range $\Delta\omega$ chosen according to the condition

$$\int_{\Delta\omega} A(\omega)\,d\omega \Big/ \int_{-\infty}^{\infty} \bar{A}(\omega)\,d\omega \geq 0.99. \qquad (4.1)$$

Calculation of the values of I and A was carried out for the process of gas expansion through a plane supersonic Laval nozzle with the parameters typical of gasdynamic CO_2 lasers: the nozzle throat height $h_* = 1.5$ mm and the area ratio $F/F_* = 38$. The profile of the supersonic part of the nozzle was represented by an arc with the circumference radius of 90 mm smoothly connected with the 2 mm radius curvature in the throat region.

4.1. *Basic laws governing the radiation of a vibrationally nonequilibrium gas expanding through a nozzle*

The i.r. radiation intensity in a vibrationally nonequilibrium supersonic flow depends markedly on the initial temperature and gas pressure in the plenum chamber [3]. Therefore, in order to ascertain the accuracy of the theoretical approach realized in the present work to determine the vibrationally nonequilibrated gas radiation intensity, a comparison was made between the theoretically calculated and experimentally measured values of I for the 4.3 and 2.7 μm CO_2 bands over a wide range of gas temperatures in the plenum chamber. The investigation results for the mixture 0.1 CO_2 + 0.4 N_2 + 0.5 He are displayed in Fig. 2. The values of radiation intensity presented are related respectively to the values of I_n found experimentally and theoretically at the minimum studied gas temperature, $T_0 = 1300$ K, and pressure, $P_0 = 4.7$ atm., in the plenum chamber. The radiation intensity of the bands under consideration was determined allowing for the spectral transmission of

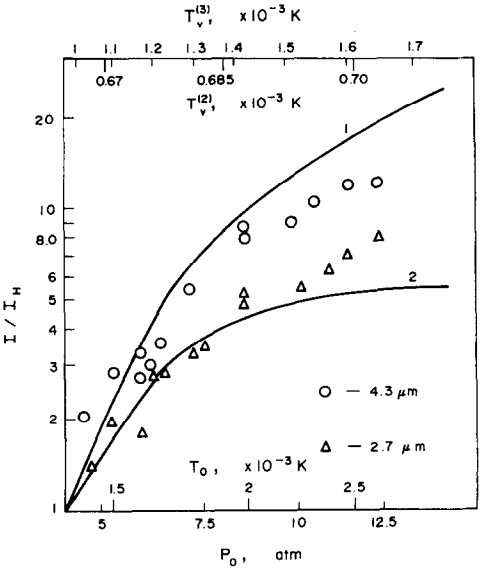

FIG. 2. Results of experimental measurements and theoretical calculation of radiation intensity in the 4.3 and 2.7 μm CO_2 bands in the supersonic flow of mixture 0.1 CO_2 + 0.4 N_2 + 0.5 He at the nozzle exit as a function of pressure, P_0, and temperature, T_0, of the gas in the plenum chamber. Curves 1 and 2 display calculation results for the 4.3 and 2.7 μm band, respectively. Calculation results of CO_2 vibrational temperatures, $T_v^{(3)}$ and $T_v^{(2)}$ at the nozzle exit are plotted on the horizontal axis in the upper part of the plot.

filters used in this study, $I = \int I(\omega)\eta(\omega)\,d\omega$, where $I(\omega)$ is the radiation intensity before the filter, $\eta(\omega)$ is its transmission function.

In the experiments, a shock tube with a supersonic nozzle mounted on the end of a low-pressure section was used. The width of the plane supersonic nozzle was 70 mm. Simultaneous recording of the radiation intensity of 4.3 and 2.7 μm bands was monitored by two identical optical systems situated symmetrically relative to the supersonic flow. Each channel consisted of a combination of a plane mirror with spherical ones focusing the flow radiation into the sensitive element of a photoresistor. In order to isolate the radiation of 4.3

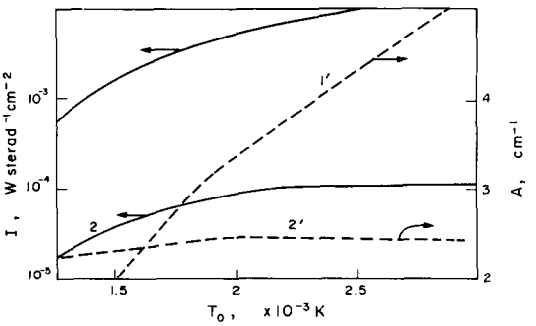

FIG. 3. Dependence of the integral radiation intensity and emissivity in the 4.3 and 2.7 μm CO_2 bands at the nozzle exit on the equilibrium gas temperature in the plenum chamber. Solid curves correspond to the radiation intensity of the bands: 1, 4.3 μm band, 2, 2.7 μm band; dashed curves, to the emissivity of: 1, 4.3 μm band; 2, 2.7 μm band emissivity increased 10-fold.

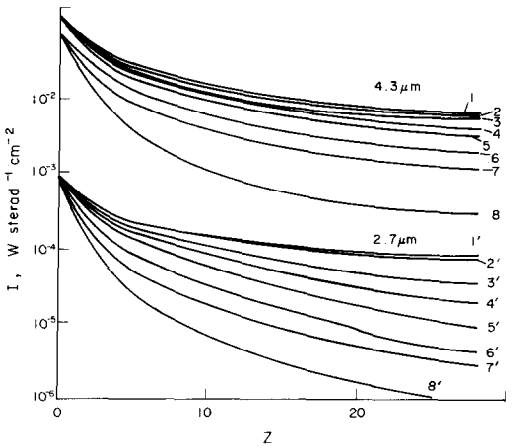

FIG. 4. Integrated radiation intensity in the 4.3 and 2.7 μm CO_2 bands of the mixtures with different water vapour content. Curves 1–8 display the calculation results on the 4.3 μm band radiation intensity, 1′–8′, on the 2.7 μm band. Curves 1, 1′ correspond to the mixture with the water vapour content, ξ_6, equal to zero; 2, 2′, to 0.001; 3, 3′, to 0.005; 4, 4′, to 0.01; 5, 5′, to 0.02; 6, 6′, to 0.05; 7, 7′, to 0.1; 8, 8′, to 0.3. The gas parameters in the plenum chamber were: $T_0 = 1800$ K $P_0 = 10.0$ atm.

and 2.7 μm bands, the filters were used having the transmission bands $\lambda = 4.37 \pm 0.06$ μm and $\lambda = 2.9 \pm 0.5$ μm, respectively.

With an increase in the gas temperature in the plenum chamber from 1300 to 3000 K, a considerable increase in radiation intensity was observed: for the 4.3 μm band, by a factor of 10–20, and for the 2.7 μm band, by about a factor of 6. This is mainly due to an increase in the vibrational temperature of CO_2 in the flow—$T_v^{(3)}$ from 1000 to 1700 K and $T_v^{(2)}$ from 660 to 720 K (Fig. 2). A larger increase of the radiation intensity of 4.3 μm band as compared with the 2.7 μm band is attributed to an increase in the vibrational

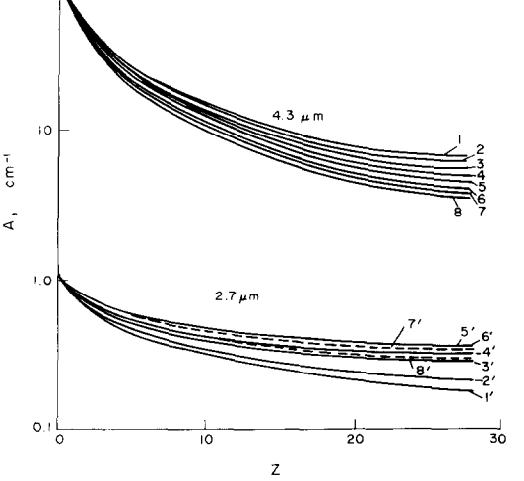

FIG. 5. Integrated emissivity in the 4.3 and 2.7 μm CO_2 bands for mixtures with different water vapour contents. Curve numbers and the initial gas parameters in the plenum chamber correspond to those in Fig. 4.

temperature of the asymmetric mode $T_v^{(3)}$ by 800 K. The radiation intensity of the 4.3 μm band is somewhat more dependent on the vibrational temperature $T_v^{(3)}$—$I_{4.3}(T_v^{(3)})$ than that of the 2.7 μm band—$I_{2.7}(T_v^{(3)})$ [66]. The vibrational temperature of the bending CO_2 mode in this case varies only slightly (by 40–50 K). This variation of $T_v^{(2)}$ has no significant effect on the radiation intensity of the bands considered.

Figure 3 displays the absolute values of integrated radiation intensity and emissivity of the 4.3 and 2.7 μm CO_2 bands calculated for the 0.1 CO_2 + 0.4 N_2 + 0.5 He mixture at the nozzle exit ($z = 21.4$) at various gas temperatures in the plenum chamber. The gas pressure before the throat was chosen constant and equal to 10.0 atm. It follows from Fig. 3 that with an increase in the gas temperature before the nozzle from 1300 to 3000 K, the radiation intensity of the 4.3 μm band in the flow at the nozzle exit increases about 20-fold, and that of the 2.7 μm band, 10-fold. Integrated emissivity of the 4.3 μm band is then increased 3-fold, of the 2.7 μm band, characterized by a much smaller radiation reabsorption, by not more than 5%. This illustrates a much stronger dependence of the radiation intensity, as compared with emissivity, on the vibrational temperature of CO_2. Therefore, in order to determine the vibrational temperatures in thermodynamically nonequilibrated supersonic flows, it is much more effective to use the measurements of the intensity of spontaneous i.r. radiation.

4.2. *The effect of water additions on the radiation intensity and emissivity of a vibrationally nonequilibrated CO_2-containing flow*

The use of the radiation intensity and emissivity measurement methods to determine the diagnostics of V–T relaxation processes in a flow was investigated with a 0.1 CO_2 + 0.9 N_2 mixture by adding to it water vapour, which markedly accelerates the processes of vibrational–translational relaxation for CO_2 and N_2 molecules [42]. The composition of mixtures studied was 0.1 CO_2 + (0.9 − ξ_6)N_2 + $\xi_6 H_2O$. The water vapour content, ξ_6, varied from 0 to 0.3. The calculations conducted show that the introduction of water vapours up to $\xi_6 = 0.3$ leads to an essential decrease of the vibrational temperatures of CO_2. The value of $T_v^{(3)}$ is diminished at the nozzle exit from 1200 to 650 K, the value of $T_v^{(2)}$, from 1000 to 400 K, while the gas temperature increases by about 100 K due to conversion of the vibrational energy of molecules into the translational one.

With the flow expansion ratio being fixed, the computations indicate that variation of the optical path length due to introduction of water molecules does not exceed 10–15%. That is why variation of radiative and absorbing properties of the gas upon introduction of water vapours is mainly attributable to a decrease in the vibrational temperatures $T_v^{(3)}$ and $T_v^{(2)}$.

Calculation results of the integral radiation intensity

of the 4.3 and 2.7 μm bands are displayed in Fig. 4. The radiation intensity of the 4.3 μm band is approximately 100 times larger than that of the 2.7 μm band. Introduction of water molecules results in a considerable decrease of the radiation intensity. An increase of the water vapour content up to $\xi_6 = 0.3$ leads to a decrease in the radiation intensity at the nozzle exit by a factor of 20 for the 4.3 μm band and by a factor of 100 for the 2.7 μm band. The greater decrease of the radiation intensity of the 2.7 μm band with introduction of water vapour is due to a strong dependence of $I_{2.7}$ on the vibrational temperature of the bending CO_2 mode which is active for this band [66]. The dependence of radiation intensity of the 4.3 μm band on the temperature $T_v^{(2)}$ is rather weak, since the bending mode in this band is passive [66].

Note that, according to the data of Fig. 4, introduction into the mixture of $\xi_6 = 0.001$ of water molecules can be reliably recorded by a diminished radiation intensity of the supersonic flow constituting $\sim 20\%$ at the nozzle exit, since the measurement error of widely used optical systems for the i.r. spectral region lies within 10–15%.

Integrated emissivity of the studied bands for expanding mixtures with different water vapour contents is presented in Fig. 5. In the course of nozzle expansion of gas, the integrated emissivity of the 4.3 μm band decreases approx. 20–50 times and of the 2.7 μm band, 4–6 times. In the region of the nozzle throat, the value of A for the 4.3 μm band is by two orders of magnitude larger than for the 2.7 μm band. At the nozzle exit, the relationship between the integral absorptions of the bands is reduced to 30–50.

Introduction of water vapours leads to a monotonous decrease of the integrated emissivity of the 4.3 μm band. For the 2.7 μm band, the dependence of the value of A on the water vapour content is of a nonmonotonous nature. The value of A somewhat increases with an increase of the water vapour content, ξ_6, from 0 to 0.05 and then decreases with a further increase of ξ_6 from 0.05 to 0.3.

In contrast to the data on variation of the integrated radiation intensity of the studied bands (Fig. 4) the integrated emissivity changes less considerably upon addition of water vapours. The increase of water vapour content, ξ_6, from 0 to 0.3 leads to a decrease of the value of A in the 4.3 μm band by no more than a factor of 2–3.

Calculation results on the spectral radiation characteristics of the 4.3 and 2.7 μm CO_2 bands with different flow expansion ratios are presented in Figs. 6(a) and (b) respectively. Radiation intensity in the central part of the 4.3 μm band is $\sim 10^{-3}$ W/(sterad cm^2 cm^{-1}) at the initial stages of flow expansion (curve 1 in Fig. 6a). In the course of expansion, the spectral radiation intensity decreases rapidly. Radiation in the central part of the 4.3 μm band at the nozzle exit ($z = 21.4$) is $\sim 6 \times 10^{-5}$ W/(sterad cm^2 cm^{-1}). In this case, narrowing of the band is observed, which is most pronounced in the long-wave region at $\lambda > 4.4$ μm. A

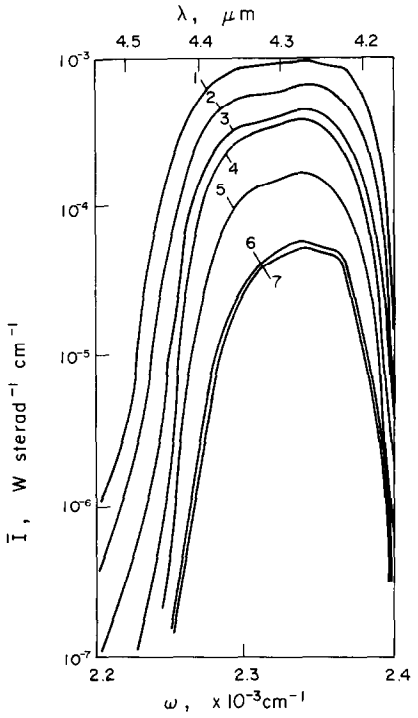

FIG. 6(a). Spectral radiation intensity in the 4.3 μm band at different expansion ratios of the mixture 0.1 CO_2 + 0.88 N_2 + 0.02 H_2O in the nozzle. Curve 1 corresponds to the value of the dimensionless parameter $z = 0.54$; 2, 1.07; 3, 2.68; 4, 5.35; 5, 10.7; 6, 21.4; 7, 25.1. The gas parameters in the plenum chamber correspond to those in Fig. 4.

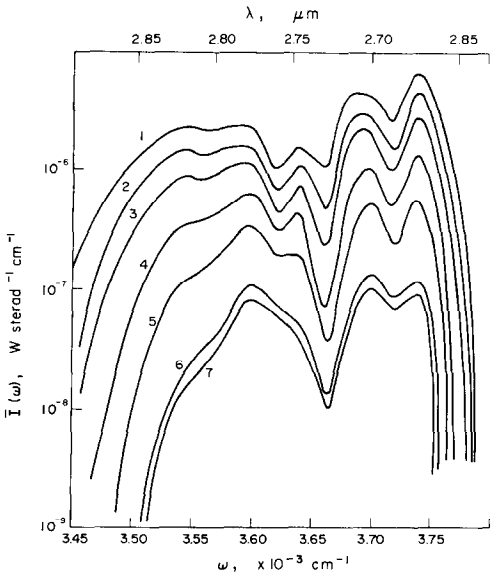

FIG. 6(b). Spectral radiation intensity in the 2.7 μm band at different expansion ratios of the mixture 0.1 CO_2 + 0.88 N_2 + 0.02 H_2O in the nozzle. Other details as Fig. 6(a).

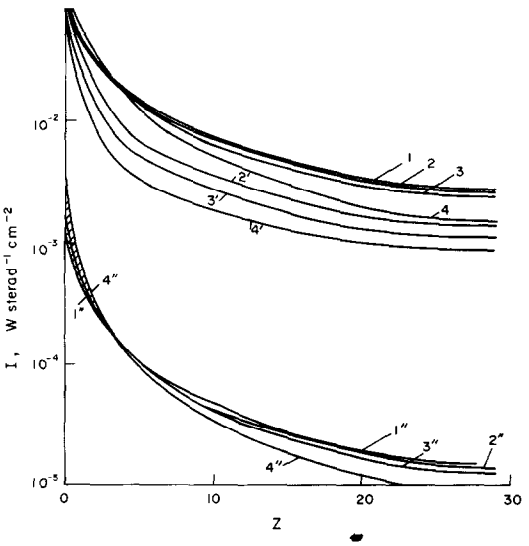

FIG. 7. Integrated radiation intensity in the 4.3 and 2.7 μm CO_2 bands and the 4.7 μm CO band during expansion of the mixtures in a nozzle depending on the carbon monoxide content. Curves 1–4 present the calculation results for the 4.3 μm band; 1′ – 4′, 4.7 μm band; 1″ – 4″, 2.7 μm band. Initial gas parameters in the plenum chamber were: T_0 = 1800 K, P_0 = 10.0 atm.

large decrease of radiation intensity in the long-wave part of the band is due to a decreasing contribution to radiation of transitions between the excited vibrational CO_2 states resulting from the processes of vibrational relaxation in the flow. Because of the anharmonicity of molecules, the intensities of vibrational transitions between the excited states are displaced towards the long-wave portion of the band.

Spectral intensity of the 2.7 μm band radiation is diminished in the course of expansion to a larger extent than that of the 4.3 μm band (Fig. 6b). Along with the above-mentioned narrowing of the long-wave part of the 4.3 μm band, a significant decrease of radiation intensity in the central part, $\lambda \approx 2.74$ μm, of the 2.7 μm band is observed. With an increasing flow expansion ratio, the 2.7 μm band is spectrally divided into two parts. This is determined by the structure of the 2.7 μm band formed by two types of vibrational transitions. The transitions with variation of vibrational quantum numbers $\Delta v_2 = 2, \Delta v_3 = 1$ emit in the long-wave part, $\lambda \gtrsim 2.74$ μm, of the 2.7 μm band, while the transitions $\Delta v_1 = \Delta v_3 = 1$, in the short-wave part, $\lambda \lesssim 2.74$ μm. Therefore, a lesser contribution to radiation of the transitions with $\Delta v_1 = \Delta v_3 = 1$ occurring between the excited vibrational states of CO_2 leads, in the course of gas expansion, to a decrease of the radiation intensity in the central part of the 2.7 μm band at λ = 2.72–2.74 μm and to the band splitting into two spectral components. A similar decrease of the contribution of transitions with $\Delta v_2 = 2$ and $\Delta v_3 = 1$ between the excited vibrational levels causes a decrease of the radiation intensity in the long-wave part of the 2.7 μm band at $\lambda \gtrsim 2.85$ μm.

4.3. *The effect of carbon monoxide substitution for nitrogen*

The possibility of determining the diagnostics of the V–V' exchange processes by means of radiative and absorbing properties of a vibrationally non-equilibrated flow has been studied using as an example the substitution of carbon monoxide for nitrogen in the mixture 0.1 CO_2 + 0.4 N_2 + 0.5 He. Introduction of carbon monoxide leads to a change in the V–V' exchange conditions of the asymmetric CO_2 mode [the processes (3.4) and (3.5)] and to the appearance of an additional channel of vibrational energy relaxation of CO_2 (v_3), N_2 and CO through the bending mode of CO_2 [process (3.7)].

The composition of the mixtures studied is described by the relationship 0.1 CO_2 + (0.4 – ξ_5)N_2 + ξ_5CO + 0.5 He. Calculations were conducted for the four mixtures corresponding to the following consecutive substitutions of carbon monoxide for nitrogen: $\xi_5 = 0$—mixture 1, 0.1—mixture 2, 0.2—mixture 3, and 0.4—mixture 4. The above numbering of mixtures is used in Figs. 7–9 to denote the calculated curves. The equilibrium gas temperature in the plenum chamber, T_0, was 1800 K, the pressure, P_0, 10.0 atm.

Calculation of the vibrational temperatures $T_v^{(2)}$, $T_v^{(3)}$, $T_v^{(5)}$ and the gas temperature T shows that introduction of carbon monoxide has a noticeable effect on the vibrational temperature of the bending mode of CO_2, $T_v^{(3)}$, and of CO, $T_v^{(5)}$. An increase in the content of CO molecules from 0 to 0.4 leads to a reduction in the vibrational temperature $T_v^{(3)}$ of about 250 K and in $T_v^{(5)}$ of 100 K in the flow at the nozzle exit. Vibrational temperature of the bending CO_2 mode, $T_v^{(2)}$, and gas temperature in the flow, T, are increased only slightly upon the introduction of carbon monoxide.

The above specific features are due to the prevailing effect of carbon monoxide on redistribution of the vibrational quanta in the system of modes $CO_2(v_3)$ + $N_2(v_4)$ + $CO(v_5)$ as compared with the effect of vibrational–translational exchange. Indeed, addition

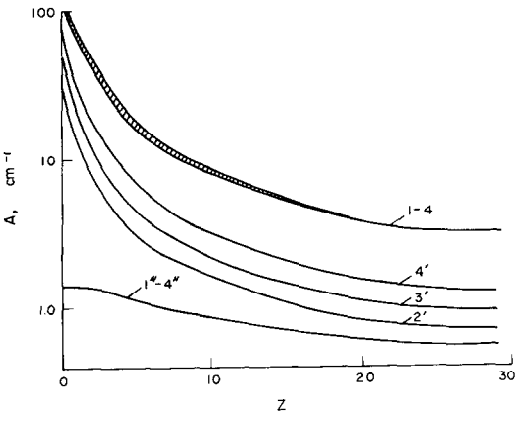

FIG. 8. Integrated emissivity in the 4.3 and 2.7 μm CO_2 bands and the 4.7 μm CO band. Curve denotations and the calculation conditions correspond to the data in Fig. 7.

of carbon monoxide molecules instead of nitrogen leads to a somewhat more rapid rate for the processes (3.2), (3.3) and (3.9) (see the data of Table 4) governing the conversion of vibrational energy into translational. The effect of helium present in the studied mixtures in the amount $\xi_7 = 0.5$ on the rates of relaxation processes is much greater than that of carbon monoxide. Thus, the effect of carbon monoxide molecules on the radiative properties of expanding flow is practically determined by the variation of the vibrational temperatures $T_v^{(3)}$ and $T_v^{(5)}$.

The calculation results on the integrated radiation intensity of the 4.3 and 2.7 μm CO_2 bands and 4.7 μm CO band in the course of expansion of mixtures 1–4 are displayed in Fig. 7. It can be seen that in an expanding flow at $z \gtrsim 1$, substitution of carbon monoxide for nitrogen leads to approximately the same decrease of radiation intensity of the 4.3 and 2.7 μm CO_2 bands. This is due to the above-mentioned decrease in the vibrational temperature, $T_v^{(3)}$, on the introduction of carbon monoxide. Radiation intensity in the 4.7 μm band in this case is increased due to an increase of the concentration of CO molecules. When the concentrations of CO_2 and CO molecules are the same and equal to 0.1 (curves 2 and 2′ in Figs. 7–8), the radiation intensity in the 4.3 μm band is 3–4 times higher than that in the 4.7 μm band. It follows from the data of Fig. 7 that the effect of carbon monoxide additions on the intensity in the 4.3 μm band in the flow at the nozzle exit can be discovered at the concentration of CO molecules $\xi_5 = 0.1$, in the 2.7 μm band at $\xi_5 = 0.2$ and in the 4.7 μm band at $\xi_5 = 0.05$.

The integrated emissivity of the considered bands at different flow expansion ratios are given in Fig. 8. It can be seen that the introduction of carbon monoxide has practically no effect on the integrated emissivity of the 4.3 and 2.7 μm bands. The integrated emissivity of the 4.7 μm band increases noticeably with the carbon monoxide content. Absorption in this band can be used to determine the effect of carbon monoxide on the vibrational distributions of CO at $\xi_5 \gtrsim 0.05$.

The dependence of the spectral radiation intensity of 4.3 and 4.7 μm bands in the mixture 0.1 CO_2 + 0.1 CO + 0.3 N_2 + 0.5 He on the flow expansion ratio is shown in Fig. 9. A marked reduction of the spectral radiation intensity is noted, which is especially large at the initial stage of expansion at $z \lesssim 3.0$ (curves 1 and 2, 1′ and 2′ in Fig. 9). At the nozzle exit ($z = 21.4$), when the process of gas expansion is practically over, radiation intensity variation is small (curves 5 and 6, 5′ and 6′ in Fig. 9). Just as in the case of introduction of water vapour, there is a more substantial radiation intensity decrease in the long-wave part of the 4.3 and 4.7 μm bands.

A considerable overlapping of the 4.3 μm CO_2 and 4.7 μm CO bands is noted in the spectral region $\lambda = 4.35$–4.50 μm, which must be taken into account when the optical systems have wide spectral transmittances.

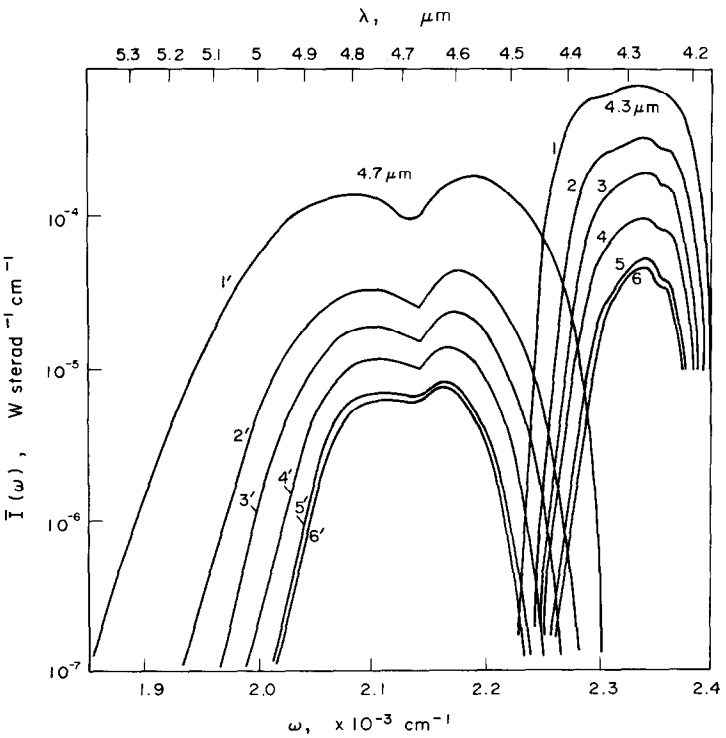

FIG. 9. Spectral radiation intensity in the 4.3 μm CO_2 band and 4.7 μm CO band at different gas expansion ratios in the nozzle. The studied mixture composition was: 0.1 CO_2 + 0.3 N_2 + 0.1 CO + 0.5 He. The gas parameters in the plenum chamber correspond to those in Fig. 7. Curves 1–6 denote the calculation results for the 4.3 μm band; 1′–6′, 4.7 μm band. Curve numbers correspond to the following values of the parameter z: 1, 1′, 0.54; 2, 2′, 2.68; 3, 3′, 5.35; 4, 4′, 10.7; 5, 5′, 21.4; 6, 6′, 32.4.

With an increase of the flow expansion ratio, the 4.3 and 4.7 μm bands are separated in the spectral region $\lambda = 4.43\ \mu$m, thus allowing their separate recording.

5. CONCLUSION

The present paper presents combined theoretical calculations of the processes of vibrational relaxation and radiative energy transfer for the case of vibrationally nonequilibrated mixtures of CO_2- and CO-containing molecular gases moving in a supersonic nozzle. The compositions of the studied mixtures and supersonic flow parameters are typical of CO_2 gasdynamic lasers. Basic regularities have been established, which determine radiation intensity and emissivity of a vibrationally nonequilibrium gas flow. The conditions have been found under which the measurement of radiation intensity in the vibrational–rotational 4.3 and 2.7 μm CO_2 bands and 4.7 μm CO band make it possible to determine reliable diagnostics for vibrational energy exchange processes. It has been shown that the effect of vibrationally nonequilibrated molecules distribution on the emissivity is relatively small, which imposes certain restrictions on the methods of absorptivity measurement in systems of this type.

Acknowledgement—The authors wish to thank R. I. Soloukhin for his continuous attention to, and interest in, these studies.

REFERENCES

1. S. A. Losev, *Gasdynamic Lasers*. Izd. Nauka, Moscow (1977).
2. J. D. Andersen, *Gasdynamic Lasers: An Introduction*. Academic Press, New York (1976).
3. N. N. Kudryavtsev, S. S. Novikov and I. B. Svetlichny, Experimental investigation of vibrational energy exchange in laser-active chemically reactive gas mixtures, Collected Papers "Khimiya Plazmy", Atomizdat, Moscow, pp. 230–278 (1980).
4. S. Brown, *Elementary Processes in a Gas Discharge Plasma*. Atomizdat, Moscow (1961).
5. V. N. Kondratiev and E. E. Nikitin, *Kinetics and Mechanism of Gas Phase Reactions*. Izd. Nauka, Moscow (1974).
6. B. F. Gordiets, A. I. Osipov and L. A. Shelepin, *Kinetic Processes in Gases and Molecular Lasers*. Izd. Nauka, Moscow (1980).
7. N. N. Kudryavtsev, S. S. Novikov and I. B. Svetlichny, The method and results of experimental determination of vibrational CO_2 temperature in nonequilibrium flows using vibrational–rotational bands models, *Dokl. Akad. Nauk SSSR* **231**, 1419–1421 (1976).
8. S. S. Penner, *Quantitative Molecular Spectroscopy and Gas Emissivities*. Addison–Wesley, London (1959).
9. R. M. Goody, *Atmospheric Radiation—I. Theoretical Basis*. Oxford University Press, London (1964).
10. C. B. Ludwig, *Handbook of Infrared Radiation from Combustion Gases*. NASA Report SP-3080, Washington (1973).
11. B. M. Smirnov and G. V. Shlyapnikov, IR radiation transfer in molecular gases, *Usp. Fiz. Nauk* **130**, 377–414 (1980).
12. V. A. Kamenshchikov, Yu. A. Plastinin, V. M. Nikolaev and L. A. Novitsky, *Radiative Properties of Gases at High Temperatures*. Izd. Mashinostroenie, Moscow (1971).
13. I. F. Golovnev, V. G. Sevostiyanenko and R. I. Soloukhin, Mathematical modelling of optical characteristics of carbon dioxide, *Inzh.-Fiz. Zh.* **36**, 197–203 (1979).
14. K. Ya. Kondratiev, Kh. Yu. Niilisk and R. Yu. Noorma, *Radiative Investigations in the Atmosphere*. Gidrometeoizdat, Leningrad (1972).
15. S. E. Gilles and W. G. Vincenti, Coupled radiative and vibrational nonequilibrium in a diatomic gas with application to gas dynamics, *Jl Quantve. Spectros. & Radiat. Transfer* **10**, 71–97 (1970).
16. K. G. P. Sulzman, Non-LTE spectral absorption coefficients for vibrational–rotational bands of diatomic molecules, *Jl Quantve. Spectros. Radiat. Transf.* **14**, 413–418 (1974).
17. V. I. Kruglov and Yu. V. Khodyko, Vibrational nonequilibrium radiation in diatomic gases, *Int. J. Heat Mass Transfer* **21**, 163–173 (1978).
18. B. A. Khmelnin and Yu. A. Plastinin, Radiative and absorbing properties of H_2O, CO_2, CO, HCl molecules at the temperatures of 300–3000 K, *Trudy TsAGI* No. 1656, 102–146 (1975).
19. R. I. Soloukhin and N. A. Fomin, Resonance (10.6 μm) absorption of CO_2 behind a shock wave, *Zh. Prinkl. Mekh. Tekh. Fiz.* No. 1 (1977).
20. R. I. Soloukhin and N. A. Fomin, Resonance absorption by carbon oxide of 9.6 μm radiation at high temperatures, *Zh. Prikl. Mekh. Tekh. Fiz.* No. 3, 3–10 (1980).
21. S. P. Vagin, S. S. Vorontsov and Yu. A. Yakobi, Infrared luminescence of CO_2-laser active medium, *Zh. Prikl. Spektr.* **29**, 621–626 (1978).
22. N. N. Kudryavtsev and S. S. Novikov, Optical method of measurement of vibrational temperatures in thermodynamically nonequilibrium gas flows, in Proceedings of the 2nd All-Union Conference on Aerophysical Investigation Techniques, Vol. 3, pp. 92–96. Izd. SO AN SSSR-AN BSSR, Novosibirsk-Minsk (1979).
23. L. P. Bakhir and Yu. V. Overchenko, Determination of vibrational level populations of CO_2 molecules in gasdynamic lasers by IR spectroscopy methods, *Zh. Prikl. Spektr.* **30**, 44–56 (1979).
24. S. Bihl, J. P. Fouassier and R. Joeckle, Calcul de l'emission infrarouge de mileux laser CO_2, *Jl Quantve. Spectros. Radiat. Transf.* **14**, 819–827 (1974).
25. S. A. Losev, On IR radiation of carbon dioxide under nonequilibrium conditions, *Nauch. Trudy Inst. Mekh. MGU* No. 43, 79–96 (1976).
26. B. I. Stepanov and V. P. Gribkovsky, *Introduction to the Theory of Luminescence*. Izd. Akad. Nauk BSSR, Minsk (1963).
27. N. N. Kudryavtsev, S. S. Novikov and I. B. Svetlichny, Experimental determination of the 001 level temperature of a carbon dioxide molecule in the nonequilibrium mixture flow of $CO_2 + N_2 + H_2$(He), *Fiz. Gor. Vzryva* **13**, 205–212 (1977).
28. C. D. Rodgers and W. Williams, Integrated absorption for Voigt profiles, *Jl. Quantve. Spectros. Radiat. Transf.* **14**, 319–326 (1974).
29. J. P. Hodgson, The nonequilibrium emissivity of carbon dioxide near 4.3 μ, *Aeronaut. Res.* Current Paper No. 1116, 3–26 (1970).
30. I. I. Ostroukhova and G. V. Shlyapnikov, Infrared radiation of a molecular gas in the Q-branch, *Teplofiz. Vysok. Temp.* **16**, 279–281 (1978).
31. G. Yamamoto, M. Tanaka and T. Aoki, Estimation of the rotational line widths of carbon dioxide bands, *Jl. Quantve. Spectros. Radiat. Transf.* **9**, 371–382 (1969).
32. P. Varanasi and S. Sarangi, Measurements of intensities and nitrogen-broadened line widths in the CO fundamental at low temperatures, *Jl. Quantve. Spectros. Radiat. Transf.* **15**, 473–483 (1975).
33. H. D. Dowling, L. R. Brown and R. H. Hunt, Line intensities of CO_2 in the 2.7 μm region, *Jl. Quantve. Spectros. Radiat. Transf.* **15**, 205–211 (1975).
34. J. P. Bouanich, Largeurs des raies spectrales de CO

autopertube at pertube par N_2, O_2, H_2, HCl, NO et CO_2, *Jl. Quantve. Spectros. Radiat. Transf.* **13,** 953–961 (1973).
35. D. A. Draegert and S. D. Williams, Collisional broadening of CO absorption lines by foreign gases, *J. Opt. Soc. Am.* **58,** 1399–1411 (1968).
36. S. R. Drayson and C. Young, Band strength and line halfwidth of the 10.4 μ CO_2 band, *Jl. Quantve. Spectros. Radiat. Transf.* **7,** 993–997 (1967).
37. M. P. Lisitsa and V. L. Strizhevsky, On temperature dependence of intensities of vibrational-rotational absorption bands of gases in the case of Fermi resonance, *Optika Spektr.* **7,** 478–484 (1959).
38. G. Hertzberg, *Molecular Spectra and Molecular Structure. I. Spectra of Diatomic Molecules.* Van Nostrand, New York (1950).
39. S. B. Petrov and M. V. Podkladenko, Investigation of broadening effects in the 4.3 μm absorption band of CO_2 over a wide temperature range, *Zh. Prikl. Spektr.* **22,** 473–476 (1975).
40. C. P. Courtoy, XII Ze spectre de $C^{12}O_2^{16}$ entre 3500 et 8000 cm^{-1} et les constantes moleculares de cette molecule, *Can. J. Phys.* **35,** 608–648 (1957).
41. N. G. Basov, V. G. Mikhailov, A. N. Oraevsky and V. A. Shcheglov, Production of inverse population in a binary gas supersonic flow in a Laval nozzle, *Zh. Tekh. Fiz.* **38,** 2031–2041 (1968).
42. R. L. Taylor and S. Bitterman, Survey of vibrational relaxation data for the processes important in the CO_2–N_2 laser system, *Rev. Mod. Phys.* **41,** 26–47 (1969).
43. R. C. Millican and D. R. White, Systematics of vibrational relaxation, *J. Chem. Phys.* **39,** 3209–3213 (1963).
44. W. Hooker and R. Millican, Shock-tube study of vibrational relaxation of carbon monoxide for the fundamental and first overtone, *J. Chem. Phys.* **38,** 214–220 (1963).
45. D. J. Miller and R. C. Millican, Vibration relaxation of carbon monoxide by nitrogen and helium down to 100 K, *J. Chem. Phys.* **53,** 3384–3385 (1970).
46. H. K. Shin, Vibration relaxation in CO–He at low temperature, *J. Chem. Phys.* **55,** 5233–5234 (1971).
47. C. W. Rosenberg, K. N. C. Bray and N. H. Pratt, Shock tube vibrational relaxation measurements: N_2 relaxation by H_2O and CO_2–N_2 V–V rate, *J. Chem. Phys.* **56,** 3230–3237 (1972).
48. M. E. Whitson and R. J. McNeal, Temperature dependence of the quenching of vibrationally excited N_2 by NO and H_2O, *J. Chem. Phys.* **66,** 2696–2702 (1977).
49. A. S. Biryukov, V. K. Konyukhov, A. I. Lukovnikov and R. I. Serikov, Vibrational energy relaxation of the (00^01) level of a CO_2 molecule, *Zh. Eksp. Teor. Fiz.* **66,** 1248–1257 (1974).
50. G. Inone and S. Tsuchiya, Vibrational relaxation of CO_2 (001) in CO_2, He, Ne, Ar in temperature range 300–140 K, *J. Phys. Soc. Japan* **38,** 870–875 (1975).
51. G. Inone and S. Tsuchiya, Vibration-to-vibration energy transfer of CO_2 (00^01) with N_2 and CO at low temperatures, *J. Phys. Soc. Japan* **39,** 479–486 (1975).
52. A. N. Vargin, V. V. Gogokhiya, V. K. Konyukhov and L. M. Pasynkova, Investigation of relaxation time of the 00^01 level of a CO_2 molecule in the mixtures with O_2 and CO, *Kvant. Elektr.* **2,** 1331–1335 (1975).
53. A. N. Vargin, V. V. Gogokhiya, V. K. Konyukhov and L. M. Pasynkova, Determination of vibrational relaxation time of the 00^01 level of a CO_2 molecule in pure CO_2 and in a mixture with H_2O, *Zh. Tekh. Fiz.* **45,** 604–608 (1975).
54. F. Heller and C. B. Moore, Relaxation of asymmetric stretching vibration of CO_2 by collisions with H_2O, D_2O and HDO, *J. Chem. Phys.* **52,** 1005–1006 (1970).
55. C. Simpson and T. Chomder, A shock tube study of vibrational relaxation in pure CO_2 and mixtures of CO_2 with inert gases nitrogen, deuterium and hydrogen, *Proc. R. Soc.* **A317,** 265–277 (1970).
56. F. Lepowtre, G. Louis and H. Mancean, Collisional relaxation in CO_2 between 180 and 400 K measured by spectrophone method, *Chem. Phys. Lett.* **48,** 509–514 (1977).
57. C. Simpson, P. D. Gait and J. M. Simme, The vibrational deactivation of the bending mode of CO_2 by O_2 and by N_2, *Chem. Phys. Lett.* **47,** 133–136 (1977).
58. D. C. Allen, T. J. Price and C. J. Simpson, Vibrational deactivation of the bending mode of CO_2 measured between 1500 and 150 K, *Chem. Phys. Lett.* **45,** 183–187 (1977).
59. Y. Sato and S. Tsuchiya, Shock-tube study of vibrational energy transfer in the CO_2–N_2 and CO_2–CO systems, *J. Phys. Soc. Japan* **33,** 1120–1131 (1972).
60. J. Taine, An optic-acoustic study of collisional vibrational relaxation in a gaseous CO_2–CO mixture, *Chem. Phys. Lett.* **41,** 297–300 (1976).
61. M. I. Buchwald and S. H. Bauer, Vibrational relaxation in CO_2 with selected collisional partners, *J. Phys. Chem.* **76,** 3108–3115 (1972).
62. A. N. Vargin, V. V. Gogokhiya, V. K. Konyukhov and L. M. Pasynkova, Rates of resonant vibrational exchange between a CO_2 molecule and N_2 and CO molecules, *Kvant. Elektr.* **3,** 216–221 (1976).
63. J. C. Stephenson and C. B. Moore, Temperature dependence of nearly resonant vibration–vibration energy transfer in CO_2 mixtures, *J. Chem. Phys.* **56,** 1295–1308 (1972).
64. L. Doyenwette, G. Mastrocinque, A. Chakroun, H. Gueguen, M. Margottin-Maclou and L. Henry, Temperature dependence of the vibrational relaxation of CO ($V > 1$) by NO, O_2 and D_2 and of the self relaxation of CO, *J. Chem. Phys.* **67,** 3360–3366 (1977).
65. D. J. Seery, On a shock-tube study of CO_2–CO vibrational energy transfer, *J. Chem. Phys.* **56,** 631–637 (1972).
66. N. N. Kudryavtsev and S. S. Novikov, On the method of vibrational temperature measurement in thermodynamically nonequilibrium gas flows, *Inzh.-Fiz. Zh.* **28,** 411–419 (1980).

APPENDIX 1

RADIATION INTENSITY OF A GAS LAYER OF HIGH TRANSPARENCY

For a gas layer of high transparency, $\bar{\tau}(\omega) \to 1$, equation (1.4) yields

$$\bar{I}(\omega)\Big|_{y=D} = \int_0^D \sum_{n,i} B_{n,i}(\omega) \frac{\partial \bar{\tau}_{n,i}(\omega)}{\partial y} \mathrm{d}y$$

$$= \sum_{n,i} B_{n,i}(\omega) \int_0^D \mathrm{d}\bar{\tau}_{n,i}(\omega)$$

$$= \sum_{n,i} B_{n,i}(\omega) \left[1 - \bar{\tau}_{n,i}(\omega)\Big|_{y=D} \right]$$

$$= \sum_{n,i} \bar{A}_{n,i}(\omega)\Big|_{y=D} B_{n,i}(\omega).$$

APPENDIX 2

RADIATION INTENSITY OF A THERMODYNAMICALLY EQUILIBRIUM GAS

Under thermodynamically equilibrium conditions, the relationship between the populations and the statistical weights of the upper and lower levels is given by:

$$g_{vJ} N_{v'J'} / g_{v'J'} N_{vJ} = \exp\left(-\frac{hc}{k} \frac{\omega}{T} \right).$$

Then the functions $B_{n,i}(\omega)$ for all vibrational–rotational transitions forming a band are

$$B_{n,i}(\omega) = B^0(\omega, T) = 2hc^2\omega^3\left[\exp\left(\frac{hc}{k}\frac{\omega}{T}\right)^{-1}\right]^{-1}.$$

Using this relationship for the functions $B_{n,i}(\omega)$, one can determine from equation (1.4) the radiation intensity of an equilibrium gas

$$\bar{I}(\omega) = B^0(\omega, T)\int_0^D \bar{\tau}(\omega)\sum_{n,i}\frac{\partial \ln \bar{\tau}_{n,i}(\omega)}{\partial y}\mathrm{d}y$$
$$= B^0(\omega, T)\int_0^D \mathrm{d}\bar{\tau}(\omega) = \bar{A}(\omega)B^0(\omega, T).$$

ETUDE THEORIQUE ET EXPERIMENTALE DU RAYONNEMENT IR DANS UN GAZ MOLECULAIRE HORS D'EQUILIBRE EN VIBRATION ET CONTENANT DU CO_2 ET DU CO

Résumé—La luminance et l'émissivité des bandes 4,3 et 2,7 μm vibration–rotation du gaz carbonique et de la bande 4,7 μm de l'oxyde de carbonique ont été numériquement calculées et expérimentalement mesurées pour un large domaine de paramètres de mélanges hors d'équilibre en vibration qui se détendent à travers une tuyère supersonique de lasers à CO_2. Une détermination théorique des caractéristiques du milieu laser CO_2 dans la région i.r., moyennées sur la structure rotationnelle, a été faite au moyen de la théorie de bande vibrationnelle–rotationnelle qui utilise des distributions d'énergie des molécules sur les niveaux vibrationnels reconstruites sur la base des calculs de la cinétique de relaxation vibrationnelle dans le mélange.

On étudie l'effet sur le rayonnement spectral et total et sur l'absorption des bandes CO_2 et CO de l'introduction dans le mélange $CO_2 + N_2$ de molécules d'eau et de la substitution de l'oxyde de carbone dans le mélange $CO_2 + N_2 + He$.

On détermine les conditions pour lesquelles des mesures de luminance ou d'émissivité rendent possibles des diagnostics de processus de relaxation vibration–translation et vibration–vibration qui sont réalisés dans un milieu laser actif.

THEORETISCHE UND EXPERIMENTELLE UNTERSUCHUNG DES IR-STRAHLUNGSAUSTAUSCHES EINES NICHT IM SCHWINGUNGS-GLEICHGEWICHT BEFINDLICHEN MOLEKULAREN GASES AUS CO_2 UND CO

Zusammenfassung—Strahlungsintensität und Emissionsvermögen des 4,3 μm- und 2,7 μm-Schwingungs- und Rotations-Bandes von CO_2 und des 4,7 μm-Bandes von CO wurden numerisch berechnet und über einen großen Parameter-Bereich der bezüglich ihrer Schwingungen im Nichtgleichgewicht befindlichen Mischungen experimentell gemessen. Die Gasmischung expandierte dabei durch eine Überschalldüse von gasdynamischen CO_2-Lasern. Die theoretische Bestimmung der Strahlungscharakteristik des aktiven Mediums des CO_2-Lasers im IR-Spektralbereich, gemittelt über die Rotationsstruktur, wurde mit der Schwingungs–Rotationsband-Theorie durchgeführt, unter Verwendung von Nicht-Gleichgewichts-Energieverteilungen der Moleküle über den Schwingungsniveaus, die auf der Berechnungsbasis der Schwingungs-Relaxations-Kinetik in der Mischung bestimmt wurden. Es wurde eine Untersuchung über den Einfluß auf die spektrale und integrale Strahlung und Absorption der betrachteten CO_2- und CO-Banden durchgeführt, indem Wassermoleküle in die $CO_2 + N_2$-Mischung zugeführt wurden, wodurch die Prozesse der V–T-Relaxation wesentlich beschleunigt werden, und durch Substitution des N_2 durch CO in der $CO_2 + N_2 + He$ – Mischung, was zu einer Änderung der Richtung im zwischenmolekularen V–V′-Austausch führt.

Es wurden die Bedingungen bestimmt, unter welchen Messungen der Strahlungsintensität und des Emissionsvermögens eine verläßliche Vorhersage von Schwingungs–Translations-und von Schwingungs Schwingungs-Relaxations-Prozessen möglich machen. Diese Prozesse treten in den aktiven Medien gasdynamischer Laser auf.

ТЕОРЕТИЧЕСКОЕ И ЭКСПЕРИМЕНТАЛЬНОЕ ИССЛЕДОВАНИЕ ПЕРЕНОСА ИК-ИЗЛУЧЕНИЯ В КОЛЕБАТЕЛЬНО-НЕРАВНОВЕСНОМ МОЛЕКУЛЯРНОМ ГАЗЕ, СОДЕРЖАЩЕМ CO_2 И CO

Аннотация—Проведены численные расчеты и экспериментальные измерения интенсивности излучения и поглощательной способности колебательно–вращательных полос 4.3 и 2.7 мкм углекислого газа и 4.7 мкм окиси углерода в широком диапазоне изменения параметров колебательно-неравновесных смесей газодинамических CO_2-лазеров, расширяющихся в сверхзвуковом сопле. Теоретическое определение усредненных по вращательной структуре радиационных характеристик активной среды CO_2-ГДЛ в ИК-области спектра осуществлялось методами теории колебательно–вращательных полос с использованием неравновесных энергетических распределений молекул по колебательным уровням, которые восстанавливались на основе расчетов кинетики колебательной релаксации в смеси.

Исследовано влияние на спектральное и интегральное излучение и поглощения рассматриваемых полос углекислого газа и окиси углерода введения в смесь $CO_2 + N_2$ молекул воды, существенно ускоряющих протекание процессов V–T релаксации, и замены в смеси $CO_2 + N_2 + He$ азота на окись углерода, что приводит к изменению протекания межмолекулярного V–V′ обмена.

Определены условия, при которых измерения интенсивности излучения или поглощательной способности позволяют осуществлять надежную диагностику процессов колебательно–поступательной и колебательно–колебательной релаксации в активных средах газодинамических лазеров.